



Article

A Two-Temperature Fractional DPL Thermoelasticity Model with an Exponential Rabotnov Kernel for a Flexible Cylinder with Changeable Properties

Ahmed E. Abouelregal ^{1,2,*} , Yazeed Alhassan ¹, Hashem Althagafi ³ and Faisal Alsharif ⁴

¹ Department of Mathematics, College of Science and Arts, Jouf University, Al-Qurayat 77455, Saudi Arabia; ynalhasan@ju.edu.sa

² Department of Mathematics, Faculty of Science, Mansoura University, Mansoura 35516, Egypt

³ Mathematics Department, Faculty of Sciences, Umm Al-Qura University, Makkah 21955, Saudi Arabia; hathagafi@uqu.edu.sa

⁴ Department of Mathematics, College of Science, Taibah University, Al-Madinah Al-Munawarah 30002, Saudi Arabia; fsharif@taibahu.edu.sa

* Correspondence: ahabogal@ju.edu.sa

Abstract: This article presents a new thermoelastic model that incorporates fractional-order derivatives of two-phase heat transfer as well as a two-temperature concept. The objective of this model is to improve comprehension and forecasting of heat transport processes in two-phase-lag systems by employing fractional calculus. This model suggests a new generalized fractional derivative that can make different kinds of singular and non-singular fractional derivatives, depending on the kernels that are used. The non-singular kernels of the normalized sinc function and the Rabotnov fractional-exponential function are used to create the two new fractional derivatives. The thermoelastic responses of a solid cylinder with a restricted surface and exposed to a moving heat flux were examined in order to assess the correctness of the suggested model. It was considered that the cylinder's thermal characteristics are dependent on the linear temperature change and that it is submerged in a continuous magnetic field. To solve the set of equations controlling the suggested issue, Laplace transforms were used. In addition to the reliance of thermal characteristics on temperature change, the influence of derivatives and fractional order was also studied by providing numerical values for the temperature, displacement, and stress components. This study found that the speed of the heat source and variable properties significantly impact the behavior of the variables under investigation. Meanwhile, the fractional parameter has a slight effect on non-dimensional temperature changes but plays a crucial role in altering the peak value of non-dimensional displacement and pressure.

Keywords: fractional thermoelastic model; moving heat flow; non-singular kernel; sinc function; Rabotnov fractional exponential kernel



Citation: Abouelregal, A.E.; Alhassan, Y.; Althagafi, H.; Alsharif, F. A Two-Temperature Fractional DPL Thermoelasticity Model with an Exponential Rabotnov Kernel for a Flexible Cylinder with Changeable Properties. *Fractal Fract.* **2024**, *8*, 182. <https://doi.org/10.3390/fractalfract8040182>

Academic Editor: Juan J. Nieto

Received: 3 February 2024

Revised: 11 March 2024

Accepted: 14 March 2024

Published: 22 March 2024



Copyright: © 2024 by the authors. Licensee MDPI, Basel, Switzerland. This article is an open access article distributed under the terms and conditions of the Creative Commons Attribution (CC BY) license (<https://creativecommons.org/licenses/by/4.0/>).

1. Introduction

Fractional calculus is a branch of mathematical analysis that applies the concepts of integration and differentiation to orders that are not integers. Fractional calculus, in contrast to classical calculus, which deals with derivatives and integrals of integer order, involves derivatives and integrals of orders that are not integers since they are fractional. This field, which has found applications in a variety of scientific and engineering-related fields, has provided a more realistic framework for describing complicated processes that involve memory effects and long-range interactions [1].

The discipline of fractional calculus remains a vibrant area of study, with continuous investigation into its various applications in domains such as physics, engineering, biology, economics, signal processing, and others. Fractional calculus is employed to mathematically represent and study intricate physical systems that encompass phenomena such as

diffusion, heat conduction, wave propagation, viscoelasticity, electrochemistry, and control systems [1]. It offers a more precise depiction of materials exhibiting memory effects, non-local behavior, and anomalous diffusion, characterized by non-random particle propagation [2]. Biological systems, including medication administration, bioelectricity, enzyme kinetics, and brain networks, may be effectively modeled using fractional calculus. It aids in capturing the intricate dynamics and enduring memory exhibited in biological systems [3]. Fractional calculus is employed in the development and examination of control systems that exhibit fractional dynamics. It facilitates the regulation of systems with memory and long-range interactions, resulting in enhanced system efficiency and stability. Fractional differential and integration are used in the analysis of viscoelastic materials, where the relationship between stress and strain is described by fractional differential equations; they are also used to simulate heat transfer in materials that exhibit memory effects and non-local interactions [4].

The presence of singular kernels in certain locations and the absence of singular kernels in other locations have significantly contributed to the growing importance and ongoing research in the field of fractional calculus [5,6]. The presence of these obstacles has stimulated extensive research endeavors and ignited enthusiasm for the advancement of novel methodologies and techniques in the realm of fractional calculus. The issue of locality occurs when employing singular kernels, such as the conventional Riemann–Liouville or Caputo derivatives. These derivatives are local operators, implying that the derivative's value at a certain place is only determined by the function's values at that point and its immediate vicinity [7]. Nevertheless, in several practical scenarios, especially those pertaining to intricate systems or substances, non-local behavior is evident, and the impact of remote sites becomes substantial. The conventional fractional derivatives are insufficient for accurately capturing this non-local behavior [8,9].

Caputo and Fabrizio [10] were the first to attempt to develop the notion of fractional calculus in this particular situation. They achieved this by presenting a non-singular integral (kernel) based on a smooth exponential function that decreases. Indeed, they did not verify the presence of a single kernel in the fractional derivative operator based on the obtained data. Conversely, they asserted that the utilization of the fractional derivative factor is suitable for a multitude of physical phenomena. In order to enhance this approach, Atanagana-Baleanu introduced a method in [11,12] that substitutes a smooth exponential function with the extended Mittag–Leffler function, which is characterized by a single parameter.

In the field of mathematical physics, general fractional-order derivatives have been utilized to investigate mathematical models. These derivatives involve the use of non-singular kernels, which include functions such as exponential, Mittag–Leffler–Gauss, Kohlrausch–Williams–Watts, Miller–Ross, Lorenzo–Hartley, Gorenflo–Mainardi, Bessel, Mittag–Leffler, Wiman, and Prabhakar that are not singular [13,14]. In the realm of fractional calculus, there is a mathematical function that is considered the Rabotnov fractional-exponential function [15]. This function is also known as the Rabotnov function. It was presented in the context of viscoelasticity and creep deformation by Nikolai Rabotnov, a Russian engineer and scientist. To describe the time-dependent behavior of viscoelastic materials, the Rabotnov function is frequently utilized. This is especially true when considering creep deformation. Both viscous (time-dependent) and elastic (time-independent) behaviors can be observed in viscoelastic materials [16]. Creep is a term that describes the slow and time-dependent deformation of a material that occurs when it is subjected to continual tension. Several other fields have discovered uses for the Rabotnov function, such as material science, engineering, and biomechanics. With its help, we can model and study how materials creep, as well as predict how they will change shape over time when loaded continuously and describe the viscoelastic properties of living tissues [17]. Engineers and scientists may be able to better understand and predict how viscoelastic materials will behave over time by adding the Rabotnov function to mathematical models. This, in turn,

facilitates the enhancement of the design and investigation of structures, gadgets, and biological systems [18].

There are two new fractional derivatives that were created by Yang et al. [19] and Yang et al. [20]. They are based on the Rabotnov fractional exponential function and the non-singular kernel with normalized sinc function. These derivatives are addressed. Because they are defined with the assistance of the normalized sinc function and the Rabotnov exponential function, both of which do not have a singular kernel, these fractional operators are quite fascinating. According to Cattani's study [21], the applications of the new FCs as well as some intriguing results may be found in the publication. In order to account for the fractal structure of the constructed material, Shymanskyi et al. [22] provided mathematical models for the issue of thermal conductivity in clay block construction. The fractal structure of the material was taken into consideration using a fractional-order integrative discriminator.

Classical thermoelasticity is a branch of continuum mechanics that combines the ideas of elasticity and heat conduction to explain how materials react to both mechanical and thermal stresses. This paradigm facilitates the analysis of the relationship between temperature and mechanical deformation in solids. An essential premise of classical thermoelasticity is the notion that the velocity of thermal disturbances is infinitely fast. This assumption suggests that every instantaneous change in temperature at a specific spot has an immediate impact on the entire material.

Hyperbolic thermoelasticity is a modified version of conventional thermoelasticity that allows for a finite thermal propagation speed instead of assuming an infinite pace. It considers the limited velocity at which thermal disruptions spread within the material. This change enables more precise simulation of processes that involve fast heat transfer or high-frequency thermal waves. In the field of hyperbolic thermoelasticity, the conventional heat transfer equation is substituted with a hyperbolic partial differential equation, commonly known as the wave equation. This equation adds a limited thermal wave speed, referred to as the speed of heat or thermal wave velocity. The wave equation incorporates the temporal lag in the spread of thermal disruptions and enables the examination of momentary thermal impacts [23].

In the context of generalized hyperbolic thermoelasticity, several extended models have been introduced in order to further improve the theory and address physical inconsistencies. Both Lord and Shulman [24] (LS) and Green and Lindsay [25] (GL) are credited with the development of the first and second generalized thermoelastic theories, respectively. Green and Naghdi [26,27] provided the most pertinent generalization of thermoelasticity, which was based on the law of entropy balance for thermal elasticity. Their idea was broken up into three distinct sections, which they referred to as GN-I, GN-II, and GN-III. Additionally, the linearized form of the GN-I theory is identical to the conventional heat transfer theory. The GN-II theory provides a fixed speed for heat propagation and does not have any energy dissipation. On the other hand, the GN-III theory allows thermal signals to propagate at both limited and unlimited velocities. Tzou [28,29] examined a constitutive equation in order to describe the logging behavior of heat transfer in materials. Tzou applied two-phase delays to both the heat flux vector and the temperature gradient, respectively. As the time of relaxation for the quick transient impacts is caused by thermal inertia, the phase lag of the heat flux vector is used as an interpretation. A delay time that is induced by the interactions between the microstructures is understood as the other phase lag of the temperature gradient.

Chen and Gurtin [30] and Chen et al. [31,32] proposed a heat transfer framework for deformable materials that incorporates two temperatures: conduction temperature and thermodynamic temperature. The difference between these two temperatures is directly related to the heat source in conditions that do not change over time. In the absence of any heat supply, the two temperatures are equal. Quintanilla [33] investigated the resolution potential, structural stability, and spatial patterns related to the concept of two temperatures (2TT). The concept of the thermoelasticity theory has been the focus of numerous

research publications over the past 20 years, leading to the development of what is today referred to as extended thermodynamics [34–37].

In recent years, there have been notable breakthroughs in the study of thermoelasticity, namely in the utilization of fractional calculus to model and evaluate heat transfer processes. Conventional heat transfer models that rely on single kernel operators have restrictions on accurately representing non-local behavior and memory influences. Furthermore, fractional calculus is used to explain anomalous diffusion in materials, which happens when temperature changes do not spread in a way that follows the rules of classical diffusion. This is especially important to keep in mind when dealing with materials that have inconsistencies or complicated structures.

This work introduces an innovative method in the realm of thermoelasticity by suggesting a comprehensive fractional heat conduction model with two temperatures. By using the non-singular kernel of the Rabotnov fraction and the Liouville–Caputo-type exponential function, we hope to make fractional operators more useful in the heat conduction equation. The proposed model considers the intricate dynamics of heat transfer in materials exhibiting memory effects, non-local behavior, and anomalous diffusion. To address the limitations of single kernel-based fractional heat conduction models, we employ the non-singular kernel of the sinc function and Rabotnov fractional–exponential function. This enables us to simulate the long-distance interactions and memory-dependent processes that occur in the actual world. Moreover, using the exponential function in the Liouville–Caputo framework enables a more precise characterization of the time-varying thermal response.

Different models of generalized thermoelasticity theories with different fractional derivative operators and constitutive equations have been used. In order to unify and clarify the relationships between different theoretical models of thermoelasticity, it is necessary to generalize and compare these frameworks. For this reason, the current study aimed to discover common characteristics, examine basic assumptions, and investigate links between different theoretical perspectives. This technique enables a more in-depth understanding of the fundamental principles that regulate partial thermal coupling and supports the establishment of reliable and comprehensive models.

This work examined the thermomagnetic reactions of a circular solid cylinder when placed in a constant axial magnetic field as a way to apply the derived model. The cylinder border is traction-free, whereas the surrounding space is subjected to a heat flow with a constant velocity. The method of the Laplace transform was utilized to solve the linked governing equations. This method makes it possible to solve the converted problem analytically while also simplifying equations. To make the numerical results easier to understand, graphs were used to show how different fields affected the simple medium and how it was different from the non-simple medium and fractional operators.

Using a fractional exponential function, like the Rabotnov function, as a kernel function for predicting thermal diffusion is very helpful, especially when it comes to figuring out the inverse Laplace transform of the fractional derivative. Optimizing and calculating fractional-order operators and parameters simplifies the modeling of thermoelasticity. Several studies have shown and explored the use of the fractional derivative with the exponential Rabotnov kernel in real-world situations [20,38]. Research has demonstrated the utility of using this fractional component in simulating various physical and other processes. Additionally, the fractional derivative with the exponential Rabotnov kernel abides by the conventional rule for the derivative of a constant function, which is zero.

Following a logical sequence, this article begins with the derivation of the model, then moves on to investigate special instances, then presents the solution methodologies, and finally concludes with a discussion of the findings after providing the numerical results. Through the use of this structure, it is possible to obtain a full grasp of the suggested model and the applications it has in thermoelasticity.

2. Derivation of the Fractional Thermoelasticity Model

This section will present a unique mathematical model of the fractional thermoelastic theory, including two temperatures. This model utilizes two distinct forms of fractional integrals to more precisely characterize the behavior of thermoelastic systems. Furthermore, this discussion will cover two novel fractional derivatives: The Yang–Gao–Tenreiro Machado–Baleanu (YGTB) derivative [19] and the Yang–Abdel–Aty–Cattani (YAC) derivative [20]. The derivatives are calculated using non-singular kernels, namely the normalized sinc function (SF) and the Rabotnov fractional–exponential function (RFEF).

2.1. Definitions of Fractional Derivatives

With respect to the function $\Psi(t) \in H^1(0, b)$, the fractional derivative of order $\alpha \in (0, 1)$ can be expressed in the Caputo sense as follows [4,5]:

$${}^C D_t^\alpha \Psi f \int_0^t \frac{1}{(t-s)^\alpha} \dot{\Psi}(s) ds, \quad t > 0. \quad (1)$$

One possible representation of the Rabotnov exponential function (REF) of order $\alpha \in \mathbb{R}^+$ with parameter $\zeta \in \mathbb{R}^+$ is the series shown below [39]:

$$\mathcal{R}_\alpha(\zeta z^\alpha) = \sum_{k=0}^{\infty} \frac{\zeta^k z^{(k+1)(\alpha+1)-1}}{\Gamma[(1+\alpha)(k+1)]}, \quad z \in \mathbb{C}. \quad (2)$$

Using the non-singular kernel of the Rabotnov fractional–exponential function, the following is the definition of the generic fractional-order derivative of the Liouville–Caputo type [20,40]:

$${}^{RFE} D_a^\alpha \Psi(t) = \int_a^t \dot{\Psi}(s) \mathcal{R}_\alpha(-\zeta(t-s)^\alpha) ds. \quad (3)$$

Some authors have recently presented a fractional differential operator that is based on the sinc function [19]. This is one of the many fascinating definitions of fractional operators that have been given. In addition to the fact that it is a confined function with gradual decay, this function is extremely well-liked in the field of signal analysis. In addition to this, it is the essential basic function that is used in the formulation of the Shannon wavelet theory [21]. The sinc fractional derivative of YGTMB can be expressed as follows [19]:

$${}^{SF} D_a^\alpha \Psi(t) = \frac{\alpha \mathcal{P}(\alpha)}{1-\alpha} \int_a^t \dot{\Psi}(s) \operatorname{sinc}\left(\frac{\alpha(t-s)}{1-\alpha}\right) ds. \quad (4)$$

In this context, the normalized sinc function is known as [19]

$$\operatorname{sinc}(t) = \frac{\sin(\pi t)}{\pi t}. \quad (5)$$

As a result of the wide range of desirable characteristics that this function possesses, it has emerged as an indispensable instrument in the fields of applied science and signal analysis. This was demonstrated, in particular, by the fact that [19]

$$\lim_{\beta \rightarrow 0} \operatorname{sinc}\left(\frac{t}{\beta}\right) = \delta(t), \quad (6)$$

where $\delta(t)$ represents the Dirac delta function.

2.2. Fractional Heat Conduction Equation

Conventional thermoelasticity relies on the Fourier law, which serves as the fundamental principle for comprehending the connection between heat transfer and temperature gradient. The equation expresses that the heat flow vector (\mathbf{F}) is directly proportional to the negative gradient of temperature ($\nabla\theta$) and may be mathematically represented as follows:

$$\mathbf{F} = -K\nabla\theta. \quad (7)$$

The conventional theory of thermoelasticity, which relies on Fourier's law, has constraints when addressing specific phenomena, such as the unbounded velocity of heat waves. In order to overcome these constraints, researchers have formulated comprehensive theories of thermoelasticity. These theories strive to offer more precise explanations of thermal phenomena and incorporate non-local and memory-dependent effects. To account for the limited speed at which heat can spread and for effects that are not local, generalized models of thermoelasticity add more constitutive equations. The dual-phase-lag theory, the three-phase-lag theory, and the fractional-order thermoelasticity theory are some of the models that may be used to classify these phenomena. In particular, the DPL model proposed by Tzou [28,29] provides a straightforward and user-friendly macroscopic representation of heat transport at microscopic levels. This makes it possible for engineering studies to provide acceptable precision. This is accomplished by introducing two thermal delays. Therefore, according to this hypothesis, Fourier's law is substituted with

$$\mathbf{F} + \tau_q \frac{\partial \mathbf{F}}{\partial t} = -K \left(1 + \tau_\theta \frac{\partial}{\partial t} \right) \nabla\theta. \quad (8)$$

The two-temperature theory, 2TT, was initially proposed in the late 1968s by Chen and Gurtin [30], as well as by Chen et al. [31,32]. The conductive temperature (φ) and the thermodynamic temperature (θ) are two different temperatures that both play a role in the process of heat conduction in a material body, according to this theory. In their hypothesis, they proposed that there is a connection between the two temperatures, which may be expressed using the formula that follows:

$$\varphi - b\nabla^2\varphi = \theta. \quad (9)$$

The parameter $b > 0$ represents a temperature differential, also known as a temperature disparity. If the condition $b = 0$ is satisfied, the two temperatures (2T) will be equal, leading to a return to the previous scenario of thermoelasticity when only one temperature is involved.

Since the 1970s, there has been a decline in interest in the 2TT; however, recent contributions have shown that this trend may be beginning to reverse itself. Quintanilla [33], for example, has proposed a version of the 2TT that is based on substituting Equation (8) with

$$\mathbf{F} + \tau_q \frac{\partial \mathbf{F}}{\partial t} = -K \left(1 + \tau_\theta \frac{\partial}{\partial t} \right) \nabla\varphi, \quad (10)$$

where the only difference is that the conductive temperature φ is substituted for θ in Equation (8).

Fractional-order thermoelasticity expands upon the conventional theory by using fractional derivatives to characterize heat conduction. Instead of assuming immediate and localized conduction, fractional derivatives take into consideration non-local and memory-dependent influences. This methodology enables a more precise representation of materials exhibiting atypical heat conduction characteristics and intricate microstructures. By including the Yang–Gao–Tenreiro Machado–Baleanu (YGTB) [19] and the Yang–Abdel–Aty–

Cattani (YAC) [20] fractional derivatives into the modified Fourier's law (10), it is possible to construct new fractional thermoelastic models that take the following formula:

$$\left(1 + \tau_q^\alpha D_t^\alpha\right) \mathbf{F} = -K(1 + \tau_\theta^\alpha D_t^\alpha) \nabla \varphi. \quad (11)$$

The notation D_t^α stands for one of the two fractional operators, YGTB and YAC. The equation that describes the conservation of energy in materials that undergo heat transfer can be written as follows:

$$\rho C_e \frac{\partial \theta}{\partial t} + T_0 \gamma \frac{\partial e}{\partial t} = -\nabla \cdot \mathbf{F} + Q. \quad (12)$$

It is possible to derive the modified version of the generalized two-temperature heat conduction theory with phase delays that incorporates fractional operators by combining Equations (11) and (12) into the following formula:

$$\left(1 + \tau_q^\alpha D_t^\alpha\right) \left[\rho C_E \frac{\partial \theta}{\partial t} + T_0 \gamma \frac{\partial e}{\partial t} - Q \right] = (1 + \tau_\theta^\alpha D_t^\alpha) (\nabla \cdot (K \nabla \varphi)). \quad (13)$$

2.3. Additional Governing System Equations

To describe the relationship between thermal stress and strain in an isotropic and homogeneous deformable material, additional basic control system equations of elasticity are used, often referred to as linear thermoelastic equations. These equations can be expressed as follows:

The constitutive equation, which is a mathematical expression that describes the linear relationship that exists between stress, strain, and heat in a material, takes the following form:

$$\mathbf{S} = \mu \left(\nabla \mathbf{U} + (\nabla \mathbf{U})^{Tr} \right) + \lambda (\nabla \cdot \mathbf{U}) \mathbf{I} - \gamma \theta \mathbf{I} \quad (14)$$

The relationships between strain and displacement can be mathematically stated as follows:

$$\mathbf{e} = \left(\nabla \mathbf{U} + (\nabla \mathbf{U})^{Tr} \right) / 2. \quad (15)$$

In solid mechanics, the relationship between applied forces, mass distribution, and resulting motion of a deformable solid is characterized by the equation of motion. The equation of motion can be expressed in general as follows:

$$(\lambda + \mu) \nabla (\nabla \cdot \mathbf{U}) + \mu \nabla^2 \mathbf{U} + \mathbf{R} - \gamma \nabla \theta = \rho \frac{\partial^2 \mathbf{U}}{\partial t^2}. \quad (16)$$

2.4. Electromagnetic Maxwell's Equations

The electromagnetic equations developed by Maxwell are a collection of basic equations that define the behavior of electric and magnetic fields, as well as the interactions between these fields and charges and currents. These equations, which the Scottish scientist James Clerk Maxwell developed in the 19th century, serve as the cornerstone of classical electromagnetism. The collection of equations that Maxwell developed often takes the form of differential equations, and it consists of four fundamental equations. The formulas for Maxwell's equations are as follows [41,42]:

$$\begin{aligned} \mathbf{J} &= \nabla \times \mathbf{h}, -\mu_0 \frac{\partial \mathbf{h}}{\partial t} = \nabla \times \mathbf{E}, \mathbf{E} = -\mu_0 \left(\frac{\partial \mathbf{U}}{\partial t} \times \mathbf{B} \right), \\ \mathbf{h} &= \nabla \times (\mathbf{U} \times \mathbf{B}), \nabla \cdot \mathbf{h} = 0. \end{aligned} \quad (17)$$

Electromagnetism makes use of a mathematical construct known as the Maxwell stress tensor, which is represented by the symbol \mathbf{M} . This tensor is used to explain the forces that are exerted on a material medium by electric and magnetic fields. As a result of electro-

magnetic fields, it is a representation of the stress or force that is exerted per unit area at a particular place inside the medium. The definition of the Maxwell stress is as follows [43]:

$$\mathbf{M} = \frac{1}{\mu_0} \left[(\nabla \cdot \mathbf{B})\mathbf{B} + (\mathbf{B} \cdot \nabla)\mathbf{B} - \frac{1}{2}\nabla(\mathbf{B} \cdot \mathbf{B}) \right]. \quad (18)$$

One of the cornerstones of electromagnetism is the Lorentz force equation, which is utilized to analyze the motion of charged particles encountered within electromagnetic fields. It is fundamental for comprehending what happens when charged particles move through electric and magnetic fields, how they act in particle accelerators, and how they interact with electromagnetic waves. To determine the Lorentz force \mathbf{L} , one can use the following formula:

$$\mathbf{L} = \mu_0(\mathbf{J} \times \mathbf{B}). \quad (19)$$

3. Applicable Problem Formulation

In the context of the proposed fractional thermoelasticity model, the problem of a long isotropic solid cylinder with radius R will be considered. The presence of a homogeneous axial magnetic field, denoted by $\vec{B} = (0, 0, B_0)$, which penetrates the cylindrical elastic medium, is taken into account. An axial heat flux was applied to the periphery of the solid cylinder. For the purpose of analysis and the nature of the problem, a cylindrical coordinate system (r, ξ, z) was used (see Figure 1). The coordinate origin is fixed at the center of the cylinder, and the z axis is aligned with the cylinder axis. Since the problem is based on the assumption that the thermoelastic interactions are symmetric about the z axis, the functions involved depend only on the radial coordinate r and the time variable t . A consideration was given to the regularity requirement, which indicates that the solutions of the fields are restricted when r tends to zero.

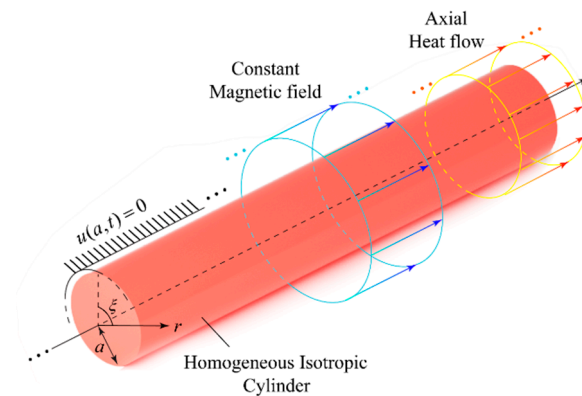


Figure 1. Geometry of a magnetically and thermally elastic solid cylinder.

In light of this, the equations that control a problem with one dimension may be expressed as

$$U_r = U(r, t), U_{\xi}(r, t) = U_z(r, t) = 0, \quad (20)$$

$$e = \frac{\partial U}{\partial r} + \frac{U}{r} = \frac{1}{r} \frac{\partial(rU)}{\partial r}, \quad (21)$$

$$S_{rr} = 2\mu \frac{\partial U}{\partial r} + \frac{\lambda}{r} \frac{\partial(rU)}{\partial r} - \gamma\theta, \quad (22)$$

$$S_{\xi\xi} = 2\mu \frac{U}{r} + \frac{\lambda}{r} \frac{\partial(rU)}{\partial r} - \gamma\theta, \quad (23)$$

$$S_{zz} = \frac{\lambda}{r} \frac{\partial(rU)}{\partial r} - \gamma\theta, \quad (24)$$

$$\frac{\partial S_{rr}}{\partial r} + \frac{1}{r}(S_{rr} - S_{\xi\xi}) + L_r = \rho \frac{\partial^2 U}{\partial t^2}. \quad (25)$$

An induced magnetic field (\vec{h}) is produced due to the interaction between the material characteristics of the cylinder and the external magnetic field surrounding it. Since it is assumed that the initial applied magnetic field \vec{B} is axial and acts parallel to the z axis, the induced magnetic field \vec{h} takes the same direction. Hence, from Equation (17), the electric current density \vec{J} and the induced electric field \vec{E} will each have a single component in the direction of the ξ orientation. As a result, we have the following relationships:

$$\vec{h} = -B_0 \left(0, 0, \frac{1}{r} \frac{\partial(rU)}{\partial r} \right), \vec{J} = B_0 \left(0, \frac{\partial}{\partial r} \left(\frac{1}{r} \frac{\partial(rU)}{\partial r} \right), 0 \right), \vec{E} = \mu_0 B_0^2 \left(0, \frac{\partial U}{\partial t}, 0 \right). \quad (26)$$

Substituting Equation (26) into Equations (18) and (19), the radial Lorentz force L_r and the stress Maxwell M_{rr} components will have the following forms:

$$L_r = \mu_0 \left(\vec{J} \times \vec{B} \right)_r = \mu_0 B_0^2 \frac{\partial}{\partial r} \left(\frac{1}{r} \frac{\partial(rU)}{\partial r} \right), M_{rr} = \mu_0 B_0^2 \left(\frac{\partial U}{\partial r} + \frac{U}{r} \right). \quad (27)$$

Matters deform and behave differently depending on their surface temperature, which is also important for several mechanical and thermal processes. The distribution of temperatures within an object affects its thermal and mechanical characteristics, which are crucial for thermoelastic material analysis and prediction.

This study assumes that the relationship between the change in temperature θ , the specific heat capacity of the material C_e , and the thermal conductivity K is a linear proportional relationship. Based on the assumption of direct proportionality between the temperature change θ , heat capacity C_e , and thermal conductivity K , they either rise or fall linearly when the temperature changes. Regardless of the fluctuation in density ρ and constant thermal expansion, we will assume the following [44,45]:

$$\begin{aligned} K(\theta) &= k_0(1 + K_1\theta), \\ C_e(\theta) &= C_{e0}(1 + K_1\theta). \end{aligned} \quad (28)$$

In this case, the reference values for specific heat capacity and thermal conductivity at a reference temperature are denoted by C_{e0} and k_0 , respectively. The rate at which these characteristics vary with temperature is determined by a constant called K_1 .

In general, the dependence of the coefficient of the specific heat capacity of the material C_e and thermal conductivity K on temperature is not always a linear function. It can display a variety of behaviors depending on the material and the temperature range it is exposed to. It is essential to keep in mind that the temperature dependence of K can vary greatly from one material to another, and even within the same material, it might display non-linear, stepwise, or other complicated behaviors to a certain extent. It is for this reason that the assumption of a linear connection between K and temperature can result in considerable inaccuracies in thermal prediction. Measurements taken in the laboratory or models that are already well known for a particular material are often utilized in order to precisely determine how the value of K varies with temperature and to incorporate its non-linear behavior into thermoelasticity models.

By utilizing Equations (9) and (28), it is possible to determine the thermal conductivity and specific heat of materials as a function of the conductive temperature as follows:

$$\begin{aligned} K &= k_0(1 + K_1(\varphi - b\nabla^2\varphi)) = k_0(1 + K_1\varphi) - k_0K_1b\nabla^2\varphi \approx k_0(1 + K_1\varphi), \\ C_e &= C_{e0}(1 + K_1(\varphi - b\nabla^2\varphi)) = C_{e0}(1 + K_1\varphi) - k_0K_1b\nabla^2\varphi \approx C_{e0}(1 + K_1\varphi). \end{aligned} \quad (29)$$

It is possible to apply the Kirchhoff transform, shown below, as a means of finding solutions:

$$\{\Theta, \Phi\} = \left\{ \frac{1}{k_0}, \frac{1}{k_0} \right\} \int_0^{\theta, \varphi} (1 + K_1 \zeta) d\zeta. \quad (30)$$

Upon applying the operator ∇ to both sides of Equation (30), we are able to derive the following:

$$k_0 \nabla \Phi = K \nabla \varphi, k_0 \nabla \Theta = K \nabla \theta. \quad (31)$$

Again, by applying the div operator ($\nabla \cdot$) to Equation (31), we can obtain the following:

$$k_0 \nabla^2 \Phi = \nabla \cdot (K \nabla \varphi), k_0 \nabla^2 \Theta = \nabla \cdot (K \nabla \theta). \quad (32)$$

On the basis of the differentiation of Equation (30) with regard to time t , we can derive

$$K_0 \frac{\partial \Theta}{\partial t} = K \frac{\partial \theta}{\partial t}. \quad (33)$$

As a result of inserting Equations (31) and (32) into Equation (13), the modified linear thermal conductivity equation with fractional order and two temperatures can be obtained as follows:

$$\nabla^2 \Phi + \tau_\theta^\alpha D_t^\alpha (\nabla^2 \Phi) = \frac{1}{k} \left(1 + \tau_q^\alpha D_t^\alpha \right) \frac{\partial \Theta}{\partial t} + \frac{\gamma T_0}{K} \left(1 + \tau_q^\alpha D_t^\alpha \right) \frac{\partial e}{\partial t}. \quad (34)$$

The parameter $k = \frac{K(\varphi)}{\rho C_e(\varphi)} = \frac{k_0}{\rho C_{e0}}$ signifies the diffusivity of the material. Material composition, microstructure, and temperature variation are a few examples of the physical parameters that affect the thermal diffusion coefficient k . Due to the requirement of Equation (28), we will assume that the thermal diffusion coefficient k is constant for the purposes of this study.

On the basis of the assumption of linearity and the substitution of Equations (31) and (32) into Equation (27), as well as the execution of a number of mathematical operations, we are able to approximate Equation (9) to obtain the following formula:

$$\Theta = (1 - b \nabla^2) \Phi. \quad (35)$$

After applying Equations (22) and (23), the equation of motion (25) may be expressed as follows:

$$\left(\frac{\lambda + 2\mu}{\rho} + \frac{\mu_0 H_0^2}{\rho} \right) \frac{\partial e}{\partial r} - \frac{\partial^2 U}{\partial t^2} = \frac{\gamma}{\rho} \frac{\partial \theta}{\partial r}. \quad (36)$$

By incorporating Equation (31) into Equation (36), we can obtain the following:

$$\left(c_1^2 + a_0^2 \right) \frac{\partial e}{\partial r} - \frac{\partial^2 U}{\partial t^2} = \frac{\gamma}{\rho(1 + K_1 \theta)} \frac{\partial \Theta}{\partial r} \quad (37)$$

where $c_1^2 = \frac{\lambda + 2\mu}{\rho}$ and $a_0^2 = \frac{\mu_0 H_0^2}{\rho}$.

After neglecting the non-linear elements in the preceding equation and making the assumption that $|\theta/T_0| \ll 1$, we are able to obtain the final result:

$$\left(c_1^2 + a_0^2 \right) \frac{\partial e}{\partial r} - \frac{\partial^2 U}{\partial t^2} = \frac{\gamma}{\rho} \frac{\partial \Theta}{\partial r}. \quad (38)$$

By introducing non-dimensional field variables, we can simplify the governing equations into non-dimensional forms. To do this, the original variables are divided by their

corresponding reference values. The following non-dimensional variables can be defined as follows:

$$\begin{aligned} \{r', U'\} &= \frac{c_1}{k} \{r, U\}, \{t', \tau'_q, \tau'_\theta\} = \frac{c_1^2}{k} \{t, \tau_q, \tau_\theta\}, K'_1 = T_0 K_1, b' = \frac{c_1^2}{k^2} b, \\ \{\theta', \varphi', \Theta', \Phi'\} &= \frac{\gamma}{\rho c_1^2} \{\theta, \varphi, \Theta, \Phi\}, \{S'_{ij}, M'_{ij}\} = \frac{1}{\rho c_1^2} \{S_{ij}, M_{rr}\}. \end{aligned} \quad (39)$$

By inserting these definitions into the governing equations and correctly measuring the other quantities involved, we may derive the non-dimensional versions of the equations as follows:

$$\left(1 + \tau_q^\alpha D_t^\alpha\right) \left(\frac{\partial \Theta}{\partial t} + \varepsilon \frac{\partial e}{\partial t}\right) (1 + \tau_\theta^\alpha D_t^\alpha) \nabla^2 \Phi, \quad (40)$$

$$\frac{\partial e}{\partial r} - a_2 \frac{\partial^2 e}{\partial t^2} = a_1 \frac{\partial \Theta}{\partial r}, \quad (41)$$

$$\Theta = (1 - b \nabla^2) \Phi, \quad (42)$$

$$S_{rr} = (1 - 2\beta^2) \frac{U}{r} + \frac{\partial U}{\partial r} - \theta, \quad (43)$$

$$S_{\xi\xi} = \frac{U}{r} + (1 - 2\beta^2) \frac{\partial U}{\partial r} - \theta, \quad (44)$$

$$S_{zz} = (1 - 2\beta^2) \frac{1}{r} \frac{\partial(rU)}{\partial r} - \theta, \quad (45)$$

where

$$\beta^2 = \frac{c_2^2}{c_1^2}, c_2^2 = \frac{\mu}{\rho}, \varepsilon = \frac{T_0 \gamma^2}{\rho^2 c_1^2 C_{e0}}, a_1 = \frac{\gamma T_0}{\rho(c_1^2 + a_0^2)}, a_2 = \frac{\rho c_1^2}{c_1^2 + a_0^2}. \quad (46)$$

In order to solve the aforementioned system of differential equations, it is possible to incorporate a new function $\Psi(r, t)$ related to the radial displacement component $U(r, t)$, commonly referred to as the potential function, in the following manner:

$$U(r, t) = \frac{\partial \Psi(r, t)}{\partial r}. \quad (47)$$

Upon substituting the suggested function Ψ into Equations (40) and (42), the following results are obtained:

$$\left(1 + \tau_q^\alpha D_t^\alpha\right) \left(\frac{\partial \Theta}{\partial t} + \varepsilon \nabla^2 \Psi\right) = (1 + \tau_\theta^\alpha D_t^\alpha) \nabla^2 \Phi, \quad (48)$$

$$\left(\nabla^2 - a_2 \frac{\partial^2}{\partial t^2}\right) \Psi = a_1 \theta. \quad (49)$$

The initial conditions are imposed as follows at time $t = 0$:

$$\begin{aligned} U(r, t) = 0 &= \frac{\partial U(r, t)}{\partial r}, \theta(r, t) = 0 = \frac{\partial \theta(r, t)}{\partial r}, \\ \Theta(r, t) = 0 &= \frac{\partial \Theta(r, 0)}{\partial r}, \Phi(r, t) = 0 = \frac{\partial \Phi(r, t)}{\partial r}. \end{aligned} \quad (50)$$

Additionally, we will take into account that for regularity requirements, the studied variables S_{ij} , M_{rr} , U , θ , Θ , φ , and Φ are constrained when $r \rightarrow 0$. This condition of regularity means that the different fields are finite when the radial distance approaches zero and do not show singularity or divergence.

A common occurrence in many manufacturing processes is the moving heat flow, a type of heat source utilized or created in machining. Thus, there are a variety of technical techniques that may be used to solve heat conduction issues with a moving heat flow, including metal cutting, welding, flame or laser hardening of metals, discharging a bullet in a rifle barrel, and more [46]. Furthermore, the relative sliding of two bodies with heat

created at the contact zone is a common feature of tribological applications and industrial processes. Moving heat flow analyzers have made it possible to characterize the temperatures produced during these operations in great detail [47].

It will be assumed that the surrounding plane of the cylinder, $r = a$, undergoes a moving heat flux denoted by F . According to the following, the fractional-order-modified Fourier law (11) will be taken into account, and we thus have the following:

$$(1 + \tau_\theta^\alpha D_t^\alpha) \left(K(\varphi) \frac{\partial \varphi}{\partial r} \right) = - (F + \tau_q^\alpha D_t^\alpha F), \text{ at } r = a. \quad (51)$$

Using Equation (31) thereafter, we obtain

$$(1 + \tau_\theta D_t^{(\alpha)}) \left(k_0 \frac{\partial \Phi}{\partial r} \right) = - (F + \tau_q D_t^{(\alpha)} F), \text{ when } t > 0, r = a. \quad (52)$$

By taking into consideration the fact that the heat flow F flows at a constant speed ϑ in the direction of the radial axis of the cylinder and decays exponentially with time, the following formula will be taken into consideration:

$$F = Q_0 e^{-\omega t} \delta(r - \vartheta t). \quad (53)$$

Given that the coefficients ω and Q_0 are considered to be constants, the Dirac delta is denoted by the symbol $\delta(\cdot)$. Through the utilization of the Dirac delta function $\delta(r - \vartheta t)$, it is guaranteed that the heat flux is concentrated in a particular region $r = \vartheta t$. We obtain the following result when we make use of the dimensionless variables (39) and then substitute them into (53):

$$(1 + \tau_\theta D_t^{(\alpha)}) \frac{\partial \Phi(r, t)}{\partial r} = -q_1 (1 + \tau_q D_t^{(\alpha)}) e^{-\omega t} \delta(r - \vartheta t), q_1 = \frac{q_0 \rho k_0 c_1}{\gamma}. \quad (54)$$

In addition to the above, we will assume that mechanical constraints ensure the restriction of surface displacement and can be expressed mathematically by the following formula:

$$U(r, t) = 0 \text{ at } r = a. \quad (55)$$

The condition sets a restriction on the mechanical response of the cylinder, ensuring that there is no displacement or distortion at the outside border. The situation can be understood as the outer surface of the cylinder being clamped or fixed, thus preventing any displacement or movement. The term usually used to describe this condition is the Dirichlet displacement boundary condition.

4. The Solution to the Problem

Due to its ability to streamline the mathematical formulation of differential equations and expedite frequency-domain solution methods, the Laplace transform is a valuable tool for differential equation analysis and solving. Differentiation, integration, and convolution may all be carried out more readily by turning the differential equations into algebraic equations in the Laplace domain. The function $g(r, t)$ is transformed using the Laplace transform, resulting in the function $\bar{g}(r, s)$. The variable s is a complex number with a positive real portion ($s > 0$). The Laplace transform is computed by utilizing the following integral:

$$\bar{g}(r, s) = \int_0^\infty g(r, t) e^{-st} dt, s > 0. \quad (56)$$

If we consider the initial conditions (50), then applying Laplace to the fundamental equations yields the following equations:

$$(\nabla^2 - \alpha_1)\bar{\Phi} = \alpha_2 \nabla^2 \bar{\Psi}, \quad (57)$$

$$(\nabla^2 - a_2 s^2)\bar{\Psi} = a_1 \bar{\Theta}, \quad (58)$$

$$\bar{\Theta} = (1 - b \nabla^2)\bar{\Phi}, \quad (59)$$

$$\bar{S}_{rr} = 2\beta^2 \frac{\partial \bar{U}}{\partial r} + (1 - 2\beta^2)\bar{e} - \bar{\theta}, \quad (60)$$

$$\bar{S}_{\xi\xi} = 2\beta^2 \frac{\bar{U}}{r} + (1 - 2\beta^2)\bar{e} - \bar{\theta}, \quad (61)$$

$$\bar{S}_{zz} = (1 - 2\beta^2)\bar{e} - \bar{\theta}, \quad (62)$$

where

$$\alpha_1 = \frac{\alpha_0}{1 + \alpha_0 b}, \quad \alpha_2 = \frac{\alpha_0 \varepsilon}{1 + \alpha_0 b}, \quad \alpha_0 = \frac{s(1 + \tau_q^\alpha \Omega(\alpha))}{(1 + \tau_\theta^\alpha \Omega(\alpha))}, \quad (63)$$

with

$$\Omega(\alpha) = \begin{cases} \frac{1}{s^{\alpha+1}} \frac{s}{1 + \xi s^{-\alpha-1}} & \text{for YAC fractional operator,} \\ \frac{\mathcal{P}(\alpha) s^2}{\pi} \tan^{-1} \left(\frac{\pi \alpha}{s(1-\alpha)} \right) & \text{for YGTB fractional operator.} \end{cases} \quad (64)$$

When the function $\bar{\Theta}$ is eliminated from Equations (57)–(59), we obtain

$$\begin{cases} (\nabla^4 - \delta_1 \nabla^2 + \delta_2)\bar{\Phi} = 0, \\ (\nabla^4 - \delta_1 \nabla^2 + \delta_2)\bar{\Psi} = 0, \end{cases} \quad (65)$$

where

$$\delta_1 = \frac{\alpha_1 + s^2 a_2 + \alpha_2 a_1}{1 + \alpha_2 a_1 b}, \quad \delta_2 = \frac{\alpha_1 s^2 a_2}{1 + \alpha_2 a_1 b}. \quad (66)$$

When we introduce the parameters μ_i , where $i = 1, 2$, into Equation (65), we obtain the following formulas:

$$\begin{cases} (\nabla^2 - \mu_1^2)(\nabla^2 - \mu_2^2)\bar{\Phi} = 0, \\ (\nabla^2 - \mu_1^2)(\nabla^2 - \mu_2^2)\bar{\Psi} = 0. \end{cases} \quad (67)$$

The coefficients μ_1^2 and μ_2^2 represent two solutions of the equation:

$$\mu^4 - \delta_1 \mu^2 + \delta_2 = 0. \quad (68)$$

The solutions for μ_1^2 and μ_2^2 can be derived by solving Equation (68) as follows:

$$\mu_1^2 = \frac{\delta_1 + \sqrt{\delta_1^2 - 4\delta_2}}{2}, \quad \mu_2^2 = \frac{\delta_1 - \sqrt{\delta_1^2 - 4\delta_2}}{2}. \quad (69)$$

The general answer to Equation (67) under the regularity condition can be expressed as follows:

$$\bar{\Phi} = \alpha_2 A_1 \mu_1^2 I_0(\mu_1 r) + \alpha_2 A_2 \mu_2^2 I_0(\mu_2 r), \quad (70)$$

$$\bar{\Psi} = (\mu_1^2 - \alpha_1) A_1 I_0(\mu_1 r) + (\mu_2^2 - \alpha_1) A_2 I_0(\mu_2 r), \quad (71)$$

where A_i , ($i = 1, 2, 3$), represents the integral parameters and $I_0(\cdot)$ represents the first class of modified Bessel functions with zero order. The following may be deduced from Equations (47) and (71):

$$\bar{U} = A_1\mu_1(\mu_1^2 - \alpha_1)I_1(\mu_1r) + \eta_2(\mu_2^2 - \alpha_1)A_2I_1(\mu_2r). \quad (72)$$

The differentiation of Equation (72) yields the following result:

$$\begin{aligned} \frac{\partial \bar{U}}{\partial r} &= A_1\mu_1^2(\mu_1^2 - \alpha_1) \left[I_0(\mu_1r) - \frac{1}{r\eta_1}I_1(\mu_1r) \right] \\ &+ A_2\mu_2^2(\mu_2^2 - \alpha_1) \left[I_0(\mu_2r) - \frac{1}{r\eta_2}I_1(\mu_2r) \right]. \end{aligned} \quad (73)$$

When entering Equation (70) into Equation (59), the function $\bar{\Theta}$ is obtained as follows:

$$\bar{\Theta} = \alpha_2\mu_1^2(1 - b\mu_1^2)A_iI_0(\mu_1r) + \alpha_2\mu_2^2(1 - b\mu_2^2)A_iI_0(\mu_2r). \quad (74)$$

If Equation (28) is substituted into Equation (30) and then integration is performed, the following conclusion may be obtained in the field of the Laplace transform:

$$\bar{\Theta} = \bar{\theta} + \frac{1}{2}K_1\bar{\theta}^2, \quad \bar{\Phi} = \bar{\varphi} + \frac{1}{2}K_1\bar{\varphi}^2. \quad (75)$$

The solutions to the aforementioned equations allow us to determine $\bar{\varphi}$ and $\bar{\theta}$ as

$$\bar{\varphi}(r, s) = \frac{1}{K_1} \left(-1 + \sqrt{1 + 2K_1\bar{\Phi}} \right), \quad (76)$$

$$\bar{\theta}(r, s) = \frac{1}{K_1} \left(-1 + \sqrt{1 + 2K_1\bar{\Theta}} \right). \quad (77)$$

Consequently, the following expressions may be used to determine the thermal stresses:

$$\begin{aligned} \bar{S}_{rr} &= A_1\mu_1^2(\mu_1^2 - \alpha_1) \left[I_0(\mu_1r) - \frac{2\beta^2}{r\mu_1}I_1(\mu_1r) \right] - \frac{-1 + \sqrt{1 + 2K_1\bar{\Theta}}}{K_1} \\ &+ A_2\mu_2^2(\mu_2^2 - \alpha_1) \left[I_0(\mu_2r) - \frac{2\beta^2}{r\mu_2}I_1(\mu_2r) \right], \end{aligned} \quad (78)$$

$$\begin{aligned} \bar{S}_{\xi\xi} &= A_1\mu_1^2(\mu_1^2 - \alpha_1) \left[(1 - 2\beta^2)I_0(\mu_1r) + \frac{2\beta^2}{r\mu_1}I_1(\mu_1r) \right] - \frac{-1 + \sqrt{1 + 2K_1\bar{\Theta}}}{K_1} \\ &+ A_2\mu_2^2(\mu_2^2 - \alpha_1) \left[(1 - 2\beta^2)I_0(\mu_2r) + \frac{2\beta^2}{r\mu_2}I_1(\mu_2r) \right], \end{aligned} \quad (79)$$

$$\begin{aligned} \bar{S}_{zz} &= A_1\mu_1^2(\mu_1^2 - \alpha_1)(1 - 2\beta^2)I_0(\mu_1r) - \frac{-1 + \sqrt{1 + 2K_1\bar{\Theta}}}{K_1} \\ &+ A_2\mu_2^2(\mu_2^2 - \alpha_1)(1 - 2\beta^2)I_0(\mu_2r). \end{aligned} \quad (80)$$

Moreover, Maxwell's stress M_{rr} has a solution that is provided by

$$\bar{M}_{rr} = \frac{a_0^2(1 - 2\beta^2)}{\alpha_2c_0^2} \left(A_1\mu_1^2(\mu_1^2 - \alpha_1)I_0(\mu_1r) + A_2\mu_2^2(\mu_2^2 - \alpha_1)I_0(\mu_2r) \right). \quad (81)$$

In the transformed domain, the boundary conditions (54) and (55) are expressed as follows:

$$\frac{\partial \bar{\Phi}(r, s)}{\partial r} = -\frac{q_1\alpha_0Q_0}{v}e^{-\Lambda r}, \Lambda = \frac{\omega + s}{v}, r = a, \quad (82)$$

$$\bar{U}(r, s) = 0, r = a. \quad (83)$$

Using Equations (70) and (72), and the boundary conditions (82) and (83), we are able to achieve the following:

$$\eta_1 A_1 I_1(\mu_1 a) + \eta_2 A_2 I_1(\mu_2 a) + \frac{\alpha_0 q_1 Q_0}{v} e^{-\Lambda a} = 0, \quad (84)$$

$$\eta_2 (\eta_1^2 - \alpha_1) A_1 I_1(\mu_1 a) + \mu_1 (\mu_2^2 - \alpha_1) A_2 I_1(\mu_2 a) = 0. \quad (85)$$

In order to obtain the parameters A_i , ($i = 1, 2$), it is necessary to solve the system of Equations (84) and (85). As a result, the issue has been resolved successfully inside the Laplace transform field.

5. Numerical Laplace Inversions

In order to obtain the displacement, stress, and temperature fields in the time domain, it is necessary to perform inverse Laplace transforms on the corresponding solutions obtained in the Laplace domain. This is particularly important for studying the problem and analyzing dynamic responses, transient phenomena, and position- and time-dependent processes. One reliable and accurate way to perform this transformation is the numerical inversion method, which is founded on the Fourier series. By using a finite sum of exponential functions, which can be efficiently computed with the help of the Fast Fourier Transform (FFT), this method involves estimating the inverse Laplace transform based on the exponential functions [48]. The accuracy of the approximation can be modified by adjusting the number of terms included in the sum as well as the time scale used in the Fourier series. When working with complex functions and systems that may not have a closed solution in the time domain, this technique is very useful because of its versatility [49].

Any field $\bar{H}(r, s)$ in the Laplace space domain can be converted to the time and space domain by utilizing the approach that is described below [50,51]:

$$H(r, t) = \frac{e^{\xi t}}{\tau_1} \left(\frac{\bar{H}(\xi)}{2} + \operatorname{Re} \sum_{k=1}^{N_0} e^{ik\pi t/\tau_1} \bar{H}(\xi + ik\pi/\tau_1) \right), \quad 0 \leq t \leq 2\tau_1 \quad (86)$$

The level of precision that is required for the inversion is a factor that should be considered when choosing the number of terms called N_0 . The parameter τ_1 is a constant that is positive and serves the purpose of determining the temporal range that the Fourier series has. The parameter N_0 is the minimum number of words that need to be chosen to fulfill the given formula:

$$e^{\xi t} \operatorname{Re} \left(e^{iN_0\pi t/\tau_1} \bar{H}(\xi + iN_0\pi/\tau_1) \right) \leq \epsilon \quad (87)$$

The coefficient ξ is an independent positive factor that must be greater than or equal to the real parts of all $\bar{H}(r, s)$ singularities. The parameter is configured to meet the specifications outlined in [51]. Numerical code was generated using the Mathematica computer programming language.

It is important to point out that in addition to the Bromwich integral approach, the Stehfest algorithm, and the Durbin method, when it comes to inverse Laplace transforms, other numerical methods can be utilized. While the choice of method is determined by the particular situation at hand and the level of precision that is sought, each method possesses its own set of advantages and disadvantages. The Fast Fourier Transform (FFT) algorithm is a numerical technique that is frequently utilized and capable of efficiently computing the Fourier transform as well as its inverse. When compared to methods that involve direct summation, it significantly reduces the computational cost, which makes it feasible to perform numerical calculations of the inverse Laplace transform.

6. Results and Discussion

This section analyzes the behavior of an endlessly elastic copper cylinder submerged in a magnetic field and subjected to a moving heat source, focusing on the numerical findings and discussion. The objective of this study is to validate the novel thermoelasticity model for the heat transfer equation, which relies on fractional operators of fractional order.

Copper is a highly adaptable metal with a diverse set of mechanical characteristics that render it appropriate for a multitude of uses. Copper is a malleable metal, allowing it to be readily molded and fashioned into many shapes and dimensions. Due to this characteristic, it is often favored for the production of wires, tubes, and sheets. Copper possesses exceptional thermal conductivity, making it a very suitable substance for deployment in heat exchangers, condensers, and several other heat transfer applications. For the purposes of numerical calculations and comparisons, the physical properties of copper that can be used are as follows [41]:

$$\begin{aligned} \{\lambda, \mu\} &= \{7.76, 3.86\} \times 10^{10} \left(\frac{\text{N}}{\text{m}^2} \right), \quad H_0 = 10^7 \left(\text{Am}^{-1} \right), \\ k_0 &= 401 \left(\frac{\text{W}}{\text{mK}} \right), \quad C_e = 386 \left(\frac{\text{Jkg}}{\text{K}} \right), \quad T_0 = 298 \text{ K}, \quad \rho = 8960 \left(\frac{\text{kg}}{\text{m}^3} \right), \\ \alpha_t &= 0.5 \times 10^{-6} \left(\frac{1}{\text{K}} \right) \mu_0 = 126 \times 10^{-8} \left(\text{Hm}^{-1} \right). \end{aligned}$$

Some physical field variables were found numerically, including Maxwell stress M_{rr} , radial and hoop thermal stresses (S_{rr} and $S_{\xi\xi}$), deformation U , dynamic temperature θ , and conductive temperature φ . These variables were found by using mathematics on copper material. Calculations were performed while varying the distance r within the range from 0 to 1, with a fixed time $t = 0.12$. In addition, the size of the heat source Q_0 was set to 1, and the frequency ω remained constant ($\omega = 1$). The numerical algorithm represented in Equation (86) was used to obtain the values of field variables under the influence of a number of different factors.

The main goal of this section is to assess the efficacy of modified fractional operators, classic fractional operators, and conventional derivatives in representing a physical phenomenon. The modified fractional operators under consideration are the Yang–Gao–Tenreiro Machado–Baleanu (YGTB) operator [19] and the Yang–Abdel–Aty–Cattani (YAC) operator [20]. Additionally, the conventional fractional operator being evaluated is the Riemann–Liouville (RL) operator. A comparison of results was performed to ascertain the advantages and disadvantages associated with each operator. The results of the proposed model will be consistent with the non-fractional two-temperature thermoelastic theory with phase delay and (2T-DPL) when the fractional order $\alpha = 1$.

A comparison of the fractional operators and the conventional derivative is being conducted with the intention of determining whether the fractional derivative is most likely to converge to the classical derivative as the order of differentiation becomes closer to 1. The proposed model allows us to observe the natural behavior of various physical domains by adjusting the fractional order α to appropriate values. The main difference between the bounded non-local fractional operators (YGTB and YAC) and the usual fractional model (RL) is evident when the numerical results with different fractional parameter values are considered. Figures 2–7 offer a quantitative depiction that highlights the disparities between fractional and conventional thermoelastic models, facilitating comprehension and comparison of their behavior. In this scenario, the values $\nu = 5$, $\tau_q = 0.2$, $\tau_\theta = 0.1$, $K_1 = -0.5$, and $b = 0.05$ are considered.

It is worth noting that based on the results and curves of different shapes, it is clear that the results obtained with the fractional derivative operator included in the thermal equation differ significantly from those obtained without it in terms of temperature, displacement, and thermal stress distributions. Thus, fractional differential operators can greatly influence the pattern and distribution of thermophysical fields in elastic materi-

als. Fractional-order values and the type of fractional operator can affect the stability and steady state of thermal and mechanical waves. The reason for this is as follows:

- Fractional differential operators create non-local and memory-dependent effects, resulting in different behaviors from traditional integer-order differential operators.
- Utilizing fractional derivative operators enables the representation of non-singular diffusion, non-local transport processes, and memory effects in diverse physical systems, such as thermal and mechanical waves in elastic materials.

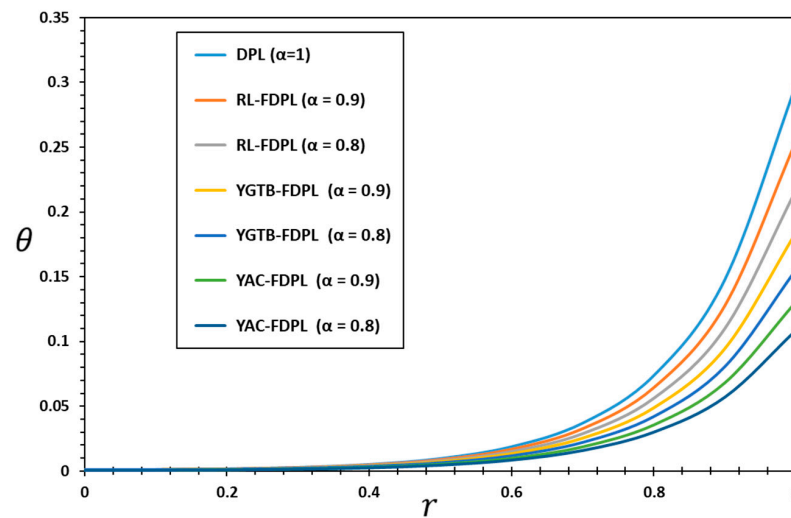


Figure 2. Dynamic temperature θ under various distinct fractional thermoelastic models.

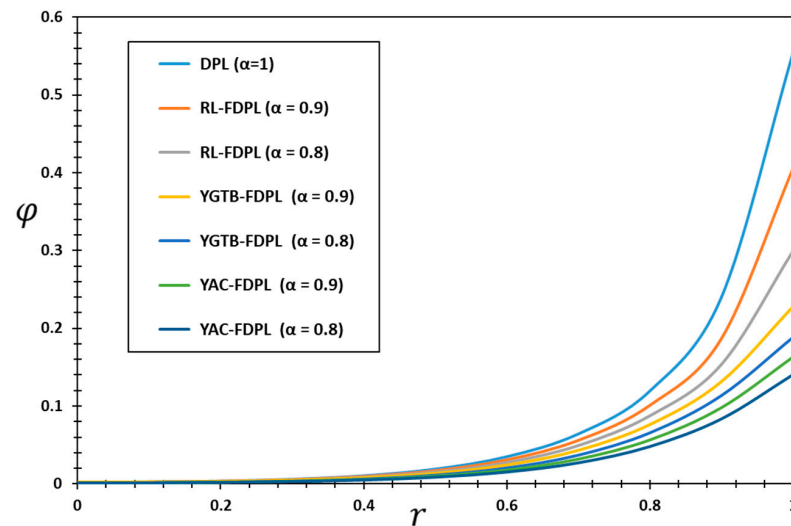


Figure 3. Conductive temperature φ under distinct fractional thermoelastic models.

Increasing the fractional order can decrease the speed at which heat waves propagate inside the medium by affecting heat flow, as demonstrated by several figures and consistent with experimental findings. The waves decay faster as they move deeper into the elastic body when the fractional-order value is decreased. The fractional order can influence the speed of wave propagation and the decay rate. This phenomenon has numerous significant applications in various domains such as thermoelasticity, viscoelasticity, and control theory. Furthermore, the fractional heat transfer wave models are capable of accurately predicting the finite velocities of heat propagation owing to the hyperbolic nature of their mathematical form.

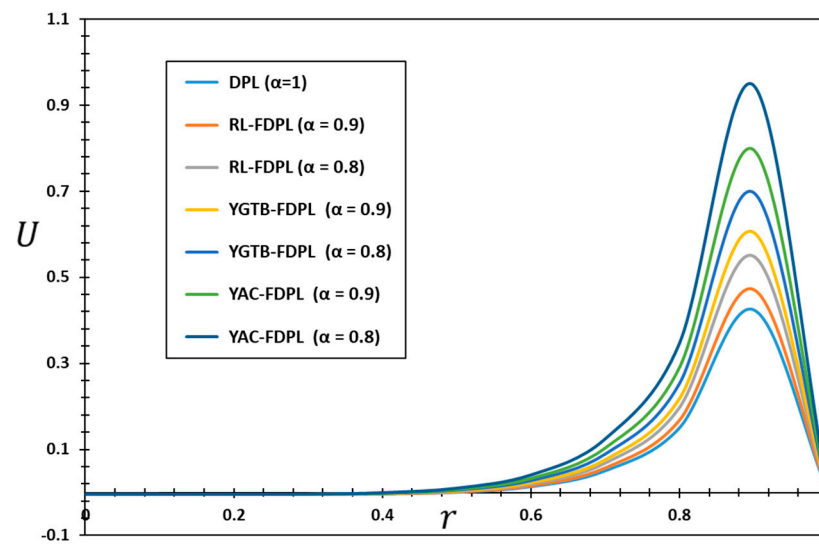


Figure 4. Displacement U under distinct fractional thermoelastic models.

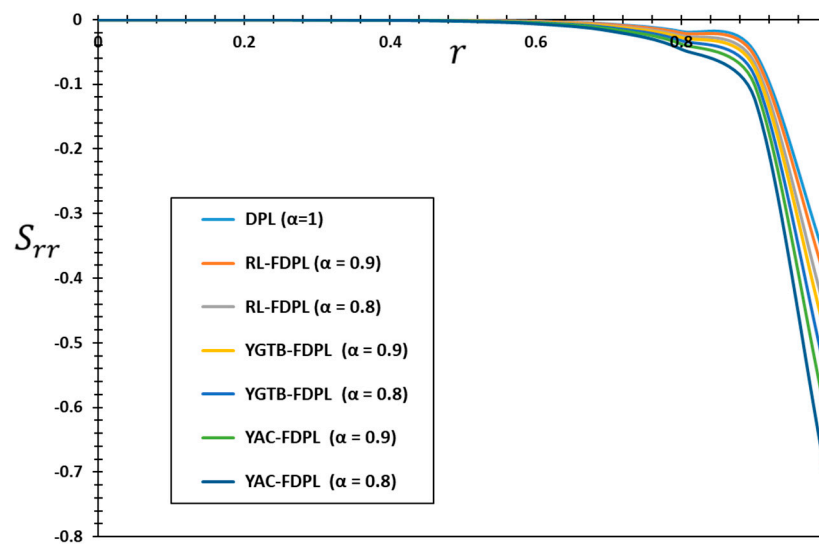


Figure 5. Radial stress S_{rr} under distinct fractional thermoelastic models.

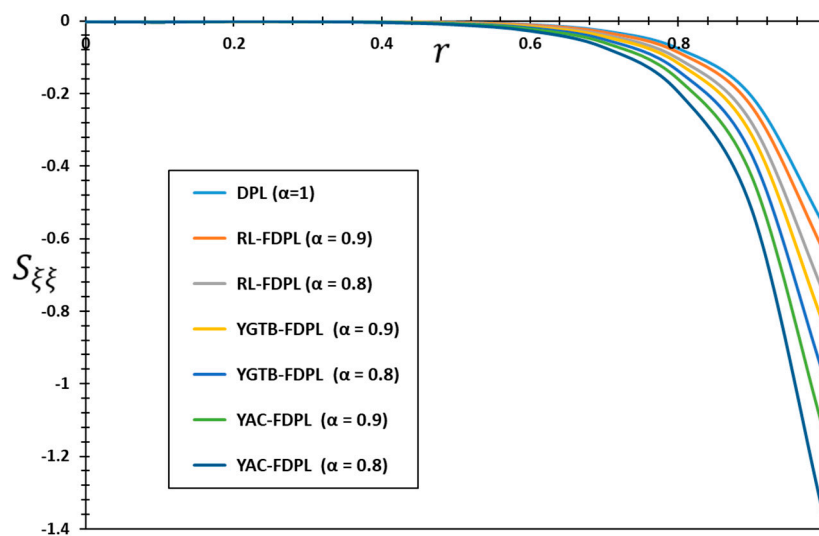


Figure 6. Hoop stress $S_{\xi\xi}$ under distinct fractional thermoelastic models.

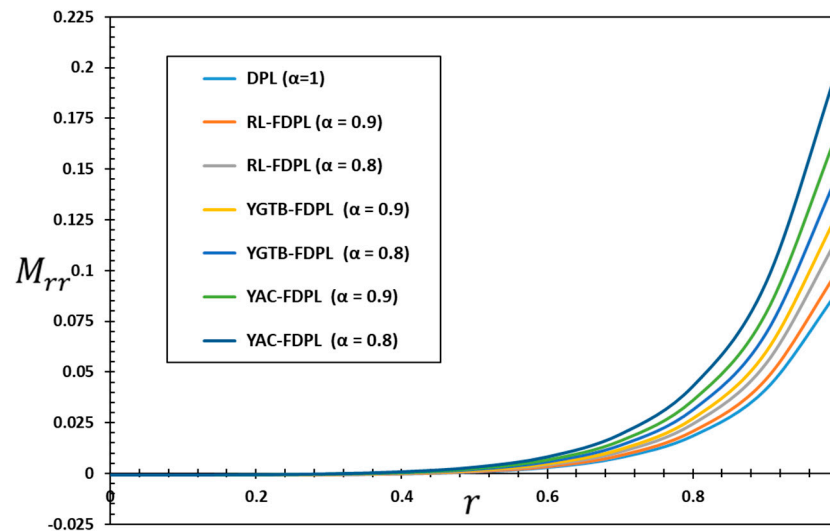


Figure 7. Maxwell's stress M_{rr} under distinct fractional thermoelastic models.

It is evident from Figures 2 and 3 that the type of differential operator (D_t^α) and the values of the fractional order (α) have a significant impact on the thermodynamic and conductivity temperatures (θ and φ). It is also clear that the surface of the cylinder ($r = 1$) experiences the largest values of the two temperatures, which then gradually decrease as they penetrate the body. The reason for this phenomenon is the constraint imposed by the fractal order (α) and delay phase times (τ_q and τ_θ) on the finite speed of heat wave propagation. On the contrary, the heat transfer equations in the case of conventional models that do not use fractional differentiation may provide an impractical result for infinite speeds of heat wave propagation. Researchers often ignore this. However, this may lead to inaccurate or impractical predictions of thermal performance in actual systems.

The figures clearly indicate that the temperature values produced using the RL operator are greater than those obtained using the fractional YGTB and YAC operators. The use of fractional differential operators (YGTB and YAC) in heat transfer models can address this limitation by providing a finite rate of heat wave propagation, which is dictated by the fractional order α . Ultimately, this could lead to enhanced accuracy and authenticity when predicting thermodynamics in complex systems, such as those in biological tissues and other materials that exhibit memory properties, such as viscous materials [52].

As a result of their ability to circumvent the singularity issues that are typically associated with conventional fractional derivative definitions, non-singular kernels are an essential component in the study of fractional calculus. Two examples of non-singular kernels that have been utilized in the study of fractional differential equations are the sinc function and the Rabotnov fractional–exponential function [53].

As shown in Figures 2–4, the existence of a heat source inhibits the zeroing of all fields under consideration, except for displacement, as distance increases. When a heat source is absent, all physical fields within a bounded region of space have non-zero values. However, beyond this region, the fields vanish indistinguishably, illustrating the finite speed of the propagation phenomenon.

Figure 4 illustrates the impact of the fractional differential parameter α on the distribution of displacement U . As the distance between the two locations within the cylinder grows, the numerical values of U progressively drop until they hit zero. The figure demonstrates that increasing the values of α results in a corresponding rise in the displacement values. This correlation may be attributed to the periodic variations in the heat source throughout time. The displacement values U on the cylinder surface are always recorded as zero where the boundary condition is met, which confirms the reliability and accuracy of the numerical results and the computational technique used. Figure 2 demonstrates that the fractional YAC thermoelastic model yields the smallest absolute displacement values,

whereas the standard fractional RL thermoelastic model yields the largest absolute displacement values. These findings indicate that the fractional YAC thermoelastic model is better suited for accurately representing the system's behavior since it yields more realistic and meaningful outcomes. Nevertheless, further examination and juxtaposition with empirical data are imperative to validate the superiority of the fractional YAC thermoelastic model in relation to other fractional models.

The numerical values in Figures 5 and 6 show that the fractional differentiation parameter α and different fractional operators (RL, YGTB, and YAC) have a significant influence on how the radial stress S_{rr} and hoop stress $S_{\xi\xi}$ propagate. The numerical values in the figures show how differences in the values of the fractional-order parameters affect the magnitudes of the thermal stresses (S_{rr} and $S_{\xi\xi}$). Depending on the type of fractional torch, pressures are likely to decrease in volume or grow in volume. The numerical results also show that large pressure values occur near the cylinder surface in the turbulent region. These pressures rapidly increase in magnitude away from the surface of the cylinder and then gradually decrease again until they completely disappear inside the elastic body.

It is also observed that thermal stresses always behave in a compressive manner near the cylinder surface in the turbulence region. In addition, it can be concluded that if fractional differentiation is included in the thermal conduction equation, the propagation of mechanical waves is reduced, consistent with physical evidence. This may be because fractional differentiation allows for the introduction of memory and genetic influences, both of which have an impact on the geographical and temporal distribution of thermal stresses. As values of the order of the fractional differential α decrease, mechanical waves travel at a slower rate and may have a shorter wavelength as a result, leading to a decrease in the propagation of mechanical waves.

The effect of the parameter and fractional operators α on the fluctuation in Maxwell stress M_{rr} is shown in Figure 7 with the change in position inside the cylinder. The figure shows that the tension decreases rapidly as the distance between them increases and shows that the action of the magnetic field is immediate and limited. Furthermore, the figure provides evidence that the fractional parameter α affects the Maxwell stress in a relatively small way. In addition, comparing the appearance and absence of fractional operators reveals the numerical values of Maxwell stresses that grow and decrease, as well as the behavior of these values. This study shows that fractional factors (α) have a significant impact on how the Maxwell stress is distributed, especially near the cylinder surface, where the variable heat source flows.

Since they can more precisely measure fractional exchanges such as thermoelasticity, fluidity, etc., new fractional derivatives can be very useful for studying the large-scale behavior of many different types of elastic materials, both simple and non-simple. This work also makes a significant contribution to the study of the finite-time propagation of thermal waves because it has implications for modern aerodynamic engineering, which uses thermoplastic cylinders. Fractional derivations are a unique technique that can help better understand the behavior of heat waves in real-world applications. The modified heat conduction equation in the suggested model can accomplish this by incorporating phase delays [54,55]. In the field of aerospace engineering, this can have major implications for the design and optimization of thermo- and viscoelastic cylinders, as well as other materials. In general, the results of this research work can provide a great addition to the topic of fractional calculus and applications of this type in the fields of engineering design and physics.

When studying fractional calculus, non-singular kernels are very important because they help avoid the problems that arise with singularities that happen with standard definitions of fractional derivatives. Various diverse non-singular kernels have been employed to investigate fractional thermophysical models. Two instances include the sinc function and the Rabotnov fractional-exponential function. We think that the YGTB- and YAC-modified fractional operators could be a good alternative to regular fractional operators and derivatives when it comes to modeling complex physical problems. This is because

they are able to simulate the behavior of the problem. These fractional operators are intriguing as they are defined using the normalized sinc function and the Rabotnov exponential function, both of which do not have a singular kernel [56]. On the other hand, further study is required in order to gain a comprehensive understanding of the benefits and drawbacks associated with these operators and to ascertain the most appropriate strategy for certain applications.

7. Conclusions

In this work, a mathematical model is presented for the thermal conductivity of homogeneous solids with specific heat and conductivity dependent on temperature change. The fractional differential operators (Riemann–Liouville, the non-singular kernel of the sine function, and the fractional exponential Rabotnov function) are all taken into account in this model. The dual-phase lag and two-temperature concepts are also considered. The use of both the non-singular sinc function and the fractional exponential Rabotnov function represents a new approach in the field of thermal theory. The model incorporates the dual-phase delay and the idea of two temperatures, enabling it to accurately represent the phase lag between thermal and mechanical reactions. The governing equations for the issue are resolved with the Laplace transform methodology. The numerical results of this study show that in addition to thermal conductivity and temperature-dependent specific heat, changes depending on the type of fractional factor and the order of fractional differentiation have a significant impact on the field variables analyzed. Below are some important notes regarding the current study:

- A large amount of impact can be exerted by fractional derivative operators on the pattern and distribution of thermophysical fields in elastic materials. Also, a significant influence on the stability and steady-state behavior of thermal and mechanical waves can be exerted by the selection of fractional-order values and the type of fractional operator.
- Accurately characterizing and forecasting the behavior of thermophysical fields in materials with memory-dependent responses requires a thorough understanding of the stability and steady-state effects as well as the modeling of those effects.
- The fractional-order parameter is a novel metric used to assess a flexible material's capacity to transfer and conduct heat, as well as other physical properties like thermal conductivity.
- By introducing non-local fractional derivatives and non-anomalous kernels, the thermal characteristics of a material can display non-local and memory-dependent impacts, leading to a more precise depiction of its features.
- The fractional derivative is able to depict heat transfer events in a manner that is consistent with experimental evidence, in contrast to the standard Fourier law of heat conduction.
- The fractional derivative operators like the Yang–Gao–Tenreiro Machado–Baleanu and Yang–Abdel–Aty–Cattani operators have proven to be effective in dealing with physical models such as thermoelasticity and viscoelasticity. Fractional derivative operators possess distinct mathematical characteristics and can represent many forms of memory-related behavior.
- This paper demonstrates how fractional calculus and operators may effectively tackle complex physical problems, thus paving the way for further research in this area. Further study and analysis of the properties and applications of fractional derivatives and operators could lead to new insights and advancements in several scientific and technical disciplines.

In the future, fractional derivatives like Riemann–Liouville (RL), Yang–Gao–Tenreiro Machado–Baleanu, and Yang–Abdel–Aty–Cattani can be further utilized to tackle emerging physical challenges. This expansion could improve our understanding and the accuracy of simulating complex physical phenomena. Choosing the right fractional derivatives

and orders is crucial for developing new models and expanding old ones in various fields such as mathematics, physics, biology, and medicine.

Author Contributions: Conceptualization, A.E.A. and Y.A.; methodology, H.A.; software, Y.A.; validation, A.E.A., F.A. and H.A.; formal analysis, H.A.; investigation, F.A.; resources, A.E.A.; data curation, Y.A. and F.A.; writing—original draft preparation, A.E.A. and H.A.; writing—review and editing, Y.A.; visualization, F.A.; supervision, H.A.; project administration, A.E.A.; funding acquisition, F.A. and Y.A. All authors have read and agreed to the published version of the manuscript.

Funding: The authors extend their appreciation to the Deputyship for Research & Innovation, Ministry of Education in Saudi Arabia for funding this research work through the project number (445-9-893).

Data Availability Statement: Data are contained within the article.

Conflicts of Interest: The authors declare no conflicts of interest.

Nomenclature

T_0	Environmental temperature	T_r	Transpose
$\gamma = (3\lambda + 2\mu)\alpha_t$	Coupling coefficient	λ, μ	Lame's elastic coefficients
\mathbf{U}	Displacement vector	Q	Heat source
\mathbf{S}	Stress tensor	\mathbf{F}	Heat flux
α	Fractional order	τ_q	Phase lag of heat flow
\mathbf{e}	Strain tensor	τ_θ	Phase lag of the temperature gradient
$\theta = T - T_0$	Temperature change	φ	Conductive temperature
ρ	Density of the material	\mathbf{h}	Induced magnetic field
T	Absolute temperature	\mathbf{E}	Induced electric field
K	Thermal conductivity	\mathbf{J}	Current density
C_e	Specific heat	\mathbf{B}	Magnetic field
α_t	Thermal expansion parameter	μ_0	Magnetic permeability
\mathbf{I}	Identity tensor	\mathbf{R}	External body force
$\Gamma(\cdot)$	Gamma function	RFEF	Rabotnov fractional–exponential function
YAC	Yang–Abdel–Aty–Cattani	YGTB	Yang–Gao–Tenreiro Machado–Baleanu
DPL	Dual-phase lag	RL	Riemann–Liouville

References

1. Tarasov, V.E. On history of mathematical economics: Application of fractional calculus. *Mathematics* **2019**, *7*, 509. [[CrossRef](#)]
2. Albers, T.; Cisternas, J.; Radons, G. Chaotic diffusion of dissipative solitons: From anti-persistent random walks to Hidden Markov Models. *Chaos Solitons Fractals* **2022**, *161*, 112290. [[CrossRef](#)]
3. Matouk, A.E. Applications of the generalized gamma function to a fractional-order biological system. *Heliyon* **2023**, *9*, e18645. [[CrossRef](#)]
4. Herrmann, R. *Fractional Calculus: An Introduction for Physicists*; World Scientific: Singapore, 2011.
5. Torres, D.F.; Malinowska, A.B. *Introduction to the Fractional Calculus of Variations*; World Scientific Publishing Company: Singapore, 2012.
6. Mainardi, F. *Fractional Calculus and Waves in Linear Viscoelasticity: An Introduction to Mathematical Models*; World Scientific: Singapore, 2022.
7. Anastassiou, G.A. *Unification of Fractional Calculi with Applications*; Springer: Cham, Switzerland, 2022; Volume 398, pp. 1–419.
8. Fernandez, A.; Baleanu, D. Classes of operators in fractional calculus: A case study. *Math. Methods Appl. Sci.* **2021**, *44*, 9143–9162. [[CrossRef](#)]
9. Saad, K.M.; Atangana, A.; Baleanu, D. New fractional derivatives with non-singular kernel applied to the Burgers equation. *Chaos Interdiscip. J. Nonlinear Sci.* **2018**, *28*, 063109. [[CrossRef](#)] [[PubMed](#)]
10. Caputo, M.; Fabrizio, M. A new definition of fractional derivative without singular kernel. *Prog. Fract. Differ. Appl.* **2015**, *1*, 73–85.

11. Atangana, A.; Baleanu, D. Caputo-Fabrizio derivative applied to groundwater flow within confined aquifer. *J. Eng. Mech.* **2017**, *143*, D4016005. [[CrossRef](#)]
12. Atangana, A.; Baleanu, D. New fractional derivatives with nonlocal and non-singular kernel: Theory and application to heat transfer model. *Therm. Sci.* **2016**, *20*, 763–769. [[CrossRef](#)]
13. Yang, X.J. *General Fractional Derivatives: Theory, Methods and Applications*; CRC Press: Boca Raton, FL, USA, 2019.
14. Singh, J.; Kumar, D.; Baleanu, D. On the analysis of chemical kinetics system pertaining to a fractional derivative with Mittag-Leffler type kernel. *Chaos Interdiscip. J. Nonlinear Sci.* **2017**, *27*, 103113. [[CrossRef](#)]
15. Rabotnov, Y. Equilibrium of an Elastic Medium with After-Effect. *Prikl. Mat. Mekhanika* **1948**, *12*, 53–62. (In Russian); Reprinted: *Fract. Calc. Appl. Anal.* **2014**, *17*, 684–696. [[CrossRef](#)]
16. Rossikhin, Y.A.; Shitikova, M.V. The fractional derivative Kelvin–Voigt model of viscoelasticity with and without volumetric relaxation. *J. Phys. Conf. Ser.* **2018**, *991*, 012069. [[CrossRef](#)]
17. Shitikova, M.V. Fractional operator viscoelastic models in dynamic problems of mechanics of solids: A review. *Mech. Solids* **2022**, *57*, 1–33. [[CrossRef](#)]
18. Popov, I.I.; Shitikova, M.V.; Levchenko, A.V.; Zhukov, A.D. Experimental identification of the fractional parameter of the fractional derivative standard linear solid model for fiber-reinforced rubber concrete. *Mech. Adv. Mater. Struct.* **2023**, *1*–9. [[CrossRef](#)]
19. Yang, X.J.; Gao, F.; Tenreiro Machado, J.A.; Baleanu, D. A new fractional derivative involving the normalized sinc function without singular kernel. *Eur. Phys. J. Spec. Top.* **2017**, *226*, 3567–3575. [[CrossRef](#)]
20. Yang, X.J.; Abdel-Aty, M.; Cattani, C. A new general fractional-order derivative with Rabotnov fractional-exponential kernel applied to model the anomalous heat transfer. *Therm. Sci.* **2019**, *23*, 1677–1681. [[CrossRef](#)]
21. Cattani, C. Sinc-fractional operator on Shannon wavelet space. *Front. Phys.* **2018**, *6*, 118. [[CrossRef](#)]
22. Shymanskyi, V.; Sokolovskyy, I.; Sokolovskyy, Y.; Bubnyak, T. Variational Method for Solving the Time-Fractal Heat Conduction Problem in the Claydite-Block Construction. In *Advances in Computer Science for Engineering and Education*; ICCSEEA 2022; Lecture Notes on Data Engineering and Communications Technologies; Hu, Z., Dychka, I., Petoukhov, S., He, M., Eds.; Springer: Cham, Switzerland, 2022; Volume 134.
23. Hetnarski, R.B.; Ignaczak, J. Generalized thermoelasticity. *J. Therm. Stress.* **1999**, *22*, 451–476.
24. Lord, H.W.; Shulman, Y. A generalized dynamical theory of thermoelasticity. *J. Mech. Phys. Solids* **1967**, *15*, 299–309. [[CrossRef](#)]
25. Green, A.E.; Lindsay, K. Thermoelasticity. *J. Elast.* **1972**, *2*, 1–7. [[CrossRef](#)]
26. Green, A.E.; Naghdi, P. Thermoelasticity without energy dissipation. *J. Elast.* **1993**, *31*, 189–208. [[CrossRef](#)]
27. Green, A.E.; Naghdi, P. On undamped heat waves in an elastic solid. *J. Therm. Stress.* **1992**, *15*, 253–264. [[CrossRef](#)]
28. Tzou, D.Y. Experimental support for the lagging behavior in heat propagation. *J. Thermophys. Heat Transf.* **1995**, *9*, 686–693. [[CrossRef](#)]
29. Tzou, D.Y. *Macro-to Microscale Heat Transfer: The Lagging Behavior*; Taylor and Francis: Washington, DC, USA, 1996.
30. Chen, P.J.; Gurtin, M.E. On a theory of heat conduction involving two temperatures. *Z. Angew. Math. Phys.* **1968**, *19*, 614–627. [[CrossRef](#)]
31. Chen, P.J.; Gurtin, M.E.; Williams, W.O. On the thermodynamics of non-simple elastic materials with two temperatures. *Z. Angew. Math. Phys.* **1969**, *20*, 107–112. [[CrossRef](#)]
32. Chen, P.J.; Williams, W.O. A note on non-simple heat conduction. *Z. Angew. Math. Phys.* **1968**, *19*, 969–970. [[CrossRef](#)]
33. Quintanilla, R. On existence, structural stability, convergence and spatial behavior in thermoelasticity with two temperatures. *Acta Mech.* **2004**, *168*, 61–73. [[CrossRef](#)]
34. Jadhav, N.B.; Gaikwad, K.R.G.; Khavale, S.G. Fractional order thermoelastic problem for a thin circular plate with uniform internal heat generation. *JP J. Heat Mass Transf.* **2023**, *35*, 107–124. [[CrossRef](#)]
35. Awad, E.; Alhazmi, S.E.; Abdou, M.A.; Fayik, M. Anomalous Thermally Induced Deformation in Kelvin–Voigt Plate with Ultra-fast Double-Strip Surface Heating. *Fractal Fract.* **2023**, *7*, 563. [[CrossRef](#)]
36. Guo, H.; Shang, F.; Tian, X.; He, T. An analytical study of transient thermo-viscoelastic responses of viscoelastic laminated sandwich composite structure for vibration control. *Mech. Adv. Mater. Struct.* **2022**, *29*, 171–181. [[CrossRef](#)]
37. Guo, H.; Shang, F.; He, T. Fractional-order rate-dependent piezoelectric thermoelasticity theory based on new fractional derivatives and its application in structural transient response analysis of smart piezoelectric composite laminates. *Int. J. Appl. Mech.* **2024**, *16*, 2450016. [[CrossRef](#)]
38. Khan, D.; Kumam, P.; Wathayu, W.; Sitthithakerngkiet, K.; Almusawa, M.Y. Application of new general fractional-order derivative with Rabotnov fractional-exponential kernel to viscous fluid in a porous medium with magnetic field. *Math. Methods Appl. Sci.* **2023**, *46*, 13457–13468. [[CrossRef](#)]
39. Qureshi, S.; Aziz, S. Fractional modeling for a chemical kinetic reaction in a batch reactor via nonlocal operator with power law kernel. *Phys. A: Stat. Mech. Appl.* **2020**, *542*, 123494. [[CrossRef](#)]
40. Yavuz, M.; Sene, N. Fundamental calculus of the fractional derivative defined with Rabotnov exponential kernel and application to nonlinear dispersive wave model. *J. Ocean. Eng. Sci.* **2021**, *6*, 196–205. [[CrossRef](#)]
41. Sadeghi, M.; Kiani, Y. Generalized magneto-thermoelasticity of a layer based on the Lord–Shulman and Green–Lindsay theories. *J. Therm. Stress.* **2022**, *45*, 319–340. [[CrossRef](#)]

42. Yadav, A.K. Reflection of plane waves in a fraction-order generalized magneto-thermoelasticity in a rotating triclinic solid half-space. *Mech. Adv. Mater. Struct.* **2022**, *29*, 4273–4290. [[CrossRef](#)]
43. Dorfmann, L.; Ogden, R.W. The nonlinear theory of magnetoelasticity and the role of the Maxwell stress: A review. *Proc. R. Soc. A* **2023**, *479*, 20230592. [[CrossRef](#)]
44. Abouelregal, A.E.; Atta, D.; Sedighi, H.M. Vibrational behavior of thermoelastic rotating nanobeams with variable thermal properties based on memory-dependent derivative of heat conduction model. *Arch. Appl. Mech.* **2023**, *93*, 197–220. [[CrossRef](#)]
45. Abouelregal, A.E.; Tiwari, R. The thermoelastic vibration of nano-sized rotating beams with variable thermal properties under axial load via memory-dependent heat conduction. *Meccanica* **2022**, *57*, 2001–2025. [[CrossRef](#)]
46. Song Wu, C.; Tsao, K.C. Modelling the three-dimensional fluid flow and heat transfer in a moving weld pool. *Eng. Comput.* **1990**, *7*, 241–248. [[CrossRef](#)]
47. Kou, S.; Hsu, S.C.; Mehrabian, R. Rapid melting and solidification of a surface due to a moving heat flux. *Metall. Trans. B* **1981**, *12*, 33–45. [[CrossRef](#)]
48. Kuhlman, K.L. Review of inverse Laplace transform algorithms for Laplace-space numerical approaches. *Numer. Algorithms* **2013**, *63*, 339–355. [[CrossRef](#)]
49. Hsu, J.T.; Dranoff, J.S. Numerical inversion of certain Laplace transforms by the direct application of fast Fourier transform (FFT) algorithm. *Comput. Chem. Eng.* **1987**, *11*, 101–110. [[CrossRef](#)]
50. Dubner, H.; Abate, J. Numerical inversion of Laplace transforms by relating them to the finite Fourier cosine transform. *J. ACM* **1968**, *15*, 115–123. [[CrossRef](#)]
51. Honig, G.; Hirdes, U. A method for the numerical inversion of Laplace transforms. *J. Comput. Appl. Math.* **1984**, *10*, 113–132. [[CrossRef](#)]
52. Khader, M.M.; Macías-Díaz, J.E.; Román-Loera, A.; Saad, K.M. A Note on a Fractional Extension of the Lotka–Volterra Model Using the Rabotnov Exponential Kernel. *Axioms* **2024**, *13*, 71. [[CrossRef](#)]
53. Kumar, S.; Nisar, K.S.; Kumar, R.; Cattani, C.; Samet, B. A new Rabotnov fractional-exponential function-based fractional derivative for diffusion equation under external force. *Math. Methods Appl. Sci.* **2020**, *43*, 4460–4471. [[CrossRef](#)]
54. Aboubakr, A.F.; Ismail, G.M.; Khader, M.M.; Abdelrahman, M.A.; AbdEl-Bar, A.M.; Adel, M. Derivation of an approximate formula of the Rabotnov fractional-exponential kernel fractional derivative and applied for numerically solving the blood ethanol concentration system. *AIMS Math.* **2023**, *8*, 30704. [[CrossRef](#)]
55. Rehman, A.U.; Riaz, M.B.; Atangana, A. Time fractional analysis of Casson fluid with Rabotnov exponential memory based on the generalized Fourier and Fick... s law. *Sci. Afr.* **2022**, *17*, e01385. [[CrossRef](#)]
56. Sehra Sadia, H.; Haq, S.U.; Khan, I. Time fractional Yang–Abdel–Cattani derivative in generalized MHD Casson fluid flow with heat source and chemical reaction. *Sci. Rep.* **2023**, *13*, 16494. [[CrossRef](#)]

Disclaimer/Publisher’s Note: The statements, opinions and data contained in all publications are solely those of the individual author(s) and contributor(s) and not of MDPI and/or the editor(s). MDPI and/or the editor(s) disclaim responsibility for any injury to people or property resulting from any ideas, methods, instructions or products referred to in the content.